The American Journal of Human Genetics, Volume *98*

Supplemental Data

RNA Interference Prevents

Autosomal-Dominant Hearing Loss

Seiji B. Shibata, Paul T. Ranum, Hideaki Moteki, Bifeng Pan, Alexander T. Goodwin, Shawn S. Goodman, Paul J. Abbas, Jeffrey R. Holt, and Richard J.H. Smith

Supplementary Materials

Supplementary Figures

Figure S1. Trans-round window membrane injection

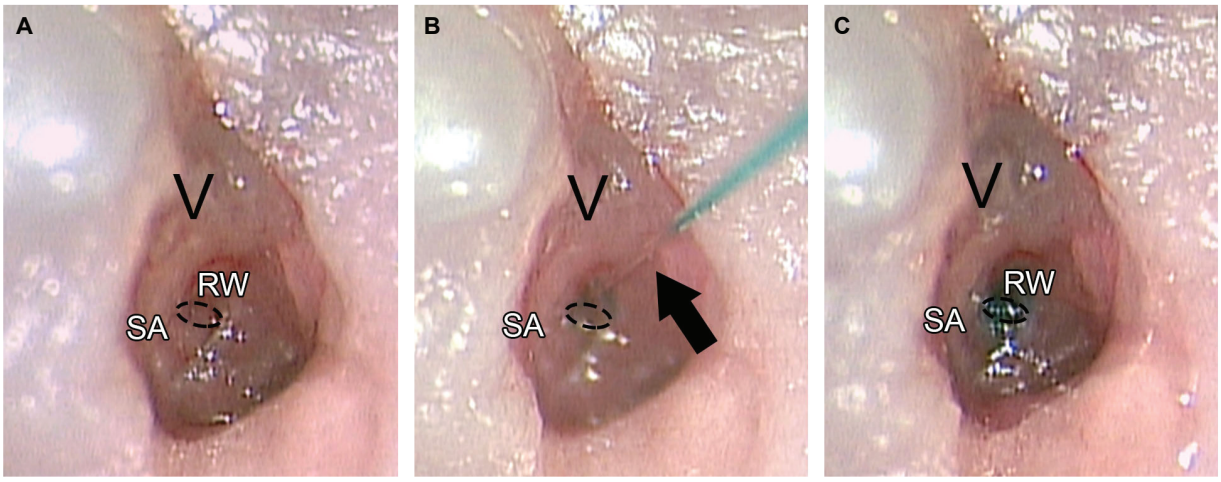

(A) Middle ear post-auricular approach in P0-P2 mice to expose and visualize the round window (RW) and stapedial artery (SA). **(B)** Pulled glass micropipette loaded with a 10:1 ratio of viral vector to 2.5% fast green dye (black arrow) used to deliver a volume of 0.5 µl through the round window membrane into the inner ear. **(C)** Faint blue coloration from the injected vector-dye mix visible in the membranous labyrinth of the cochlea and vestibule (V).

Figure S2. Comparison of calibration methods

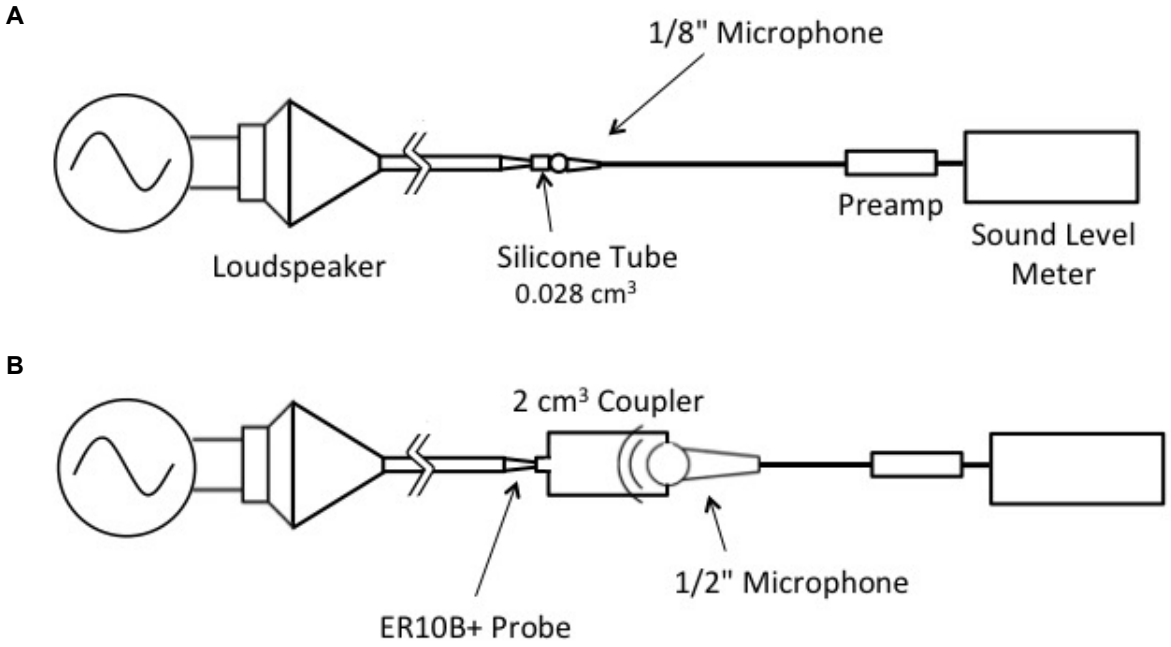

(A) Loudspeaker connected to a small cavity (0.028cm^3) that approximates the dimensions of the mouse ear canal. (**B)** Loudspeaker connected to a standard 2cm^3 cavity. For comparison measurements, loudspeakers are driven by a constant voltage.

Figure S3: rAAV2/9miTmck412.16eGFP (miTmc) transduction efficiency

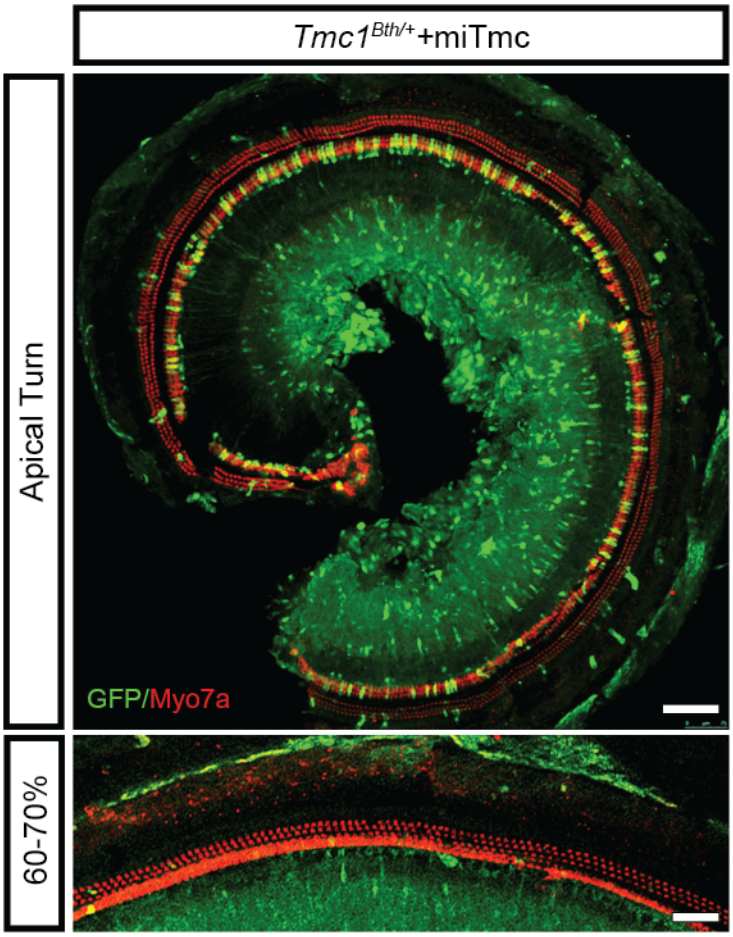

Whole mount from 2-week-old miTmc-treated cochlea injected at P0-P2. Transduction efficiency is greatest in the apical turn and less efficient in the basal turns of the cochlea as measured by GFP expression. Whole mounts were labeled with anti-Myo7a (red) to visualize hair cells. Green fluorescence comes solely from CMV-driven eGFP expression. No additional staining was used to detect GFP. Scale bars represent 50μm.

Figure S4: Control click and pure tone ABRs

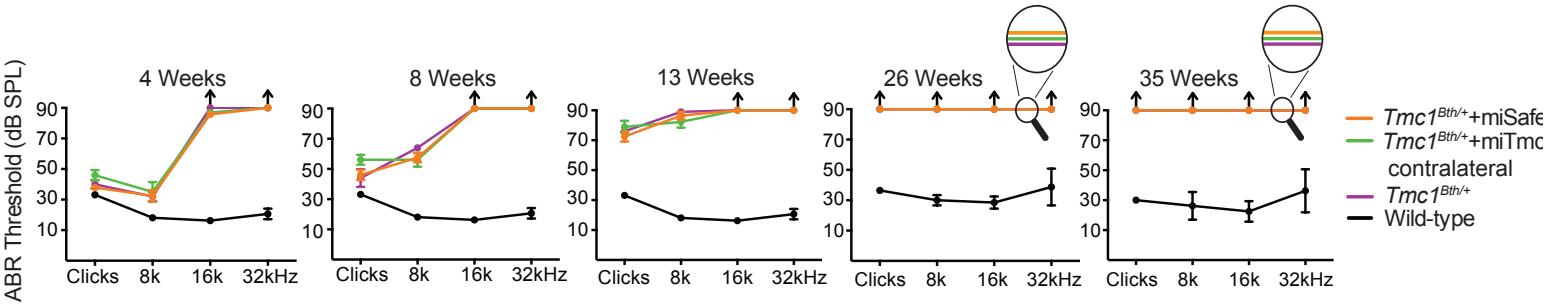

ABR thresholds from control animals follow a very similar hearing loss time course from 4 to 35 weeks. Mouse strains tested include untreated wild-type mice (black), *Tmc1*$^{Bth/+}$ mice (purple), the untreated *Tmc1*$^{Bth/+}$+miTmc contralateral ears (green), and miSafe-treated *Tmc1*$^{Bth/+}$ mice (orange). We observed no differences between thresholds of *Tmc1*$^{Bth/+}$ +miSafe mice and untreated *Tmc1*$^{Bth/+}$+miTmc contralateral groups, indicating that delivery of the AAV-packaged miRNA construct does not have a negative effect on auditory function as measured by ABR. Error bars indicate SEM. Magnifying glass indicates that multiple values share the same ABR thresholds. Wild type n=4 from 4-13 weeks and n=5 from 26 to 35 weeks; *Tmc1*$^{Bth/+}$ n=11; *Tmc1*$^{Bth/+}$+miTmc contralateral n=10; *Tmc1*$^{Bth/+}$+miSafe n=13. Black arrows indicate no response at equipment limits.

Figure S5: ABR waveforms at 35 weeks

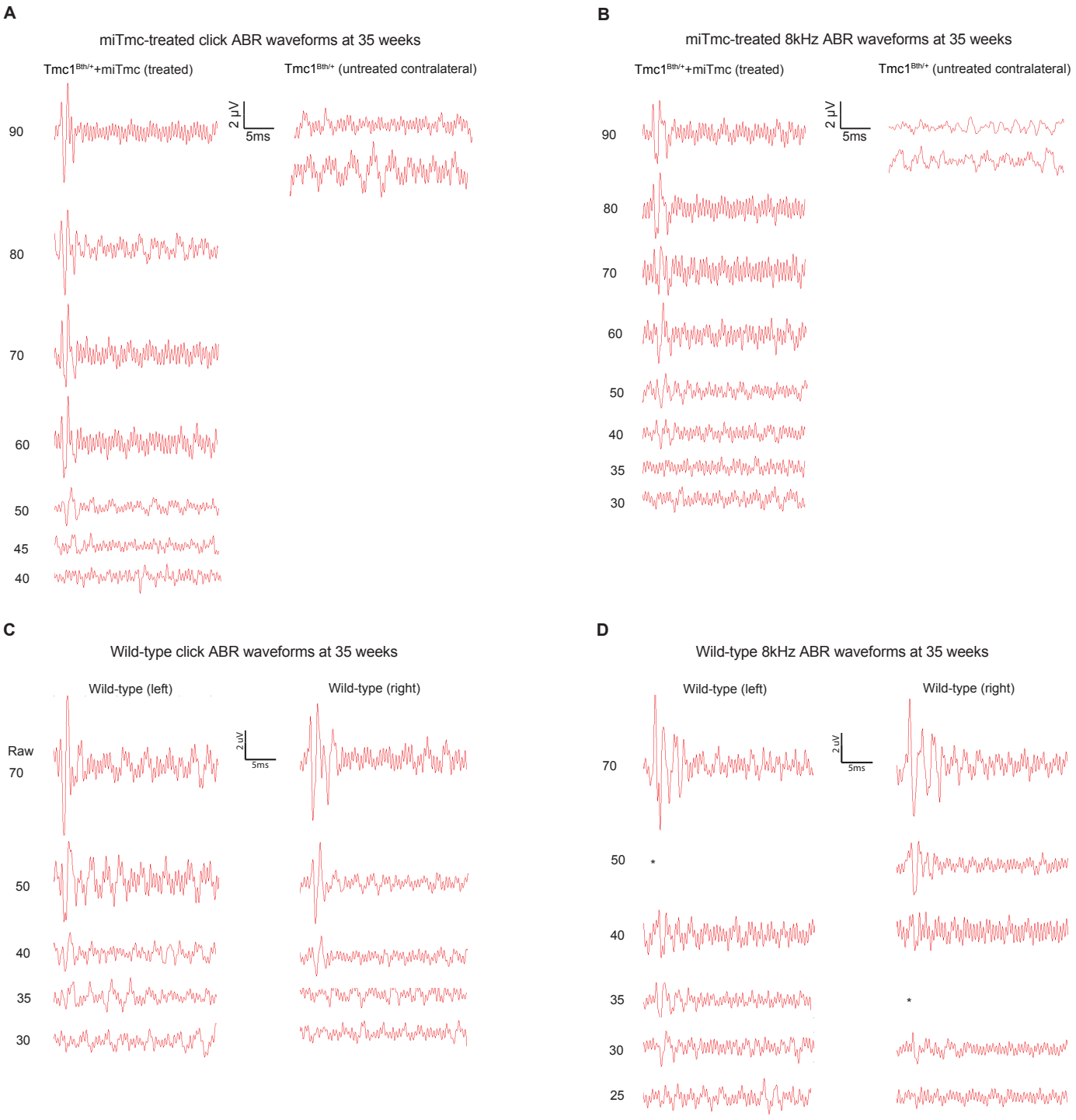

(A) Click and **(B)** 8kHz tone burst ABR waveforms measured at 35 weeks in one of the two best-performing *Tmc1*$^{Bth/+}$ +miTmc mice: left ear, treated ear; right ear, untreated contralateral ear.

Responses at the indicated sound pressure levels (dB SPL) are shown next to each trace. In the right (untreated contralateral ears), no response was observed in repetitions of click and 8kHz tone-burst ABRs at the maximum sound pressure. (C) Click and (D) 8kHz tone burst ABR waveforms from both ears of wild-type C3HeB/FeJ inbred mice.

Figure S6: ABR wave I amplitudes

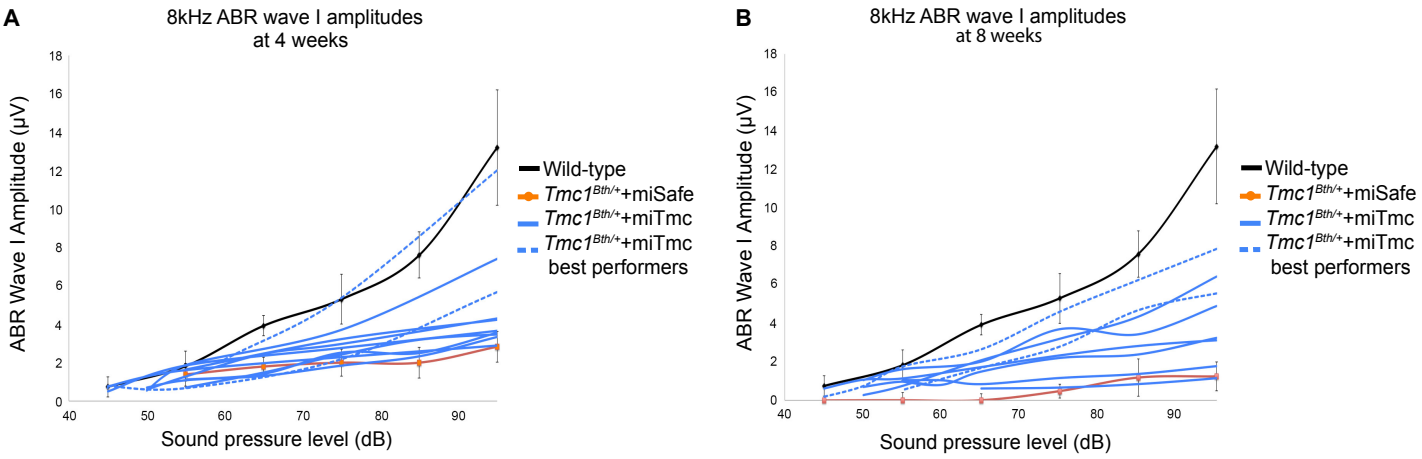

Wave I amplitudes from 8kHz ABRs at 4 (**A)** and 8 weeks (**B**) graphed for each animal in the miTmc-treated cohort and compared to the mean value of wild-type and *Tmc1*$^{Bth/+}$+miSafe mice. The dashed lines represent the top performers of *Tmc1*$^{Bth/+}$+miTmc. The peak-to-nadir wave I amplitude was used; error bars are SD. At 4 weeks, the treated left ears in *Tmc1*$^{Bth/+}$+miTmc mice had overall smaller amplitudes compared to wild-type littermate controls. *Tmc1*$^{Bth/+}$+miTmc amplitudes were more robust compared to *Tmc1*$^{Bth/+}$+miSafe amplitudes. At 8 weeks, amplitudes in *Tmc1*$^{Bth/+}$+miSafe mice continued to dampen, although in the *Tmc1*$^{Bth/+}$+miTmc mice they did not changed.

Figure S7: Stereocilia morphology in the best and worst performing miTmc-treated animals

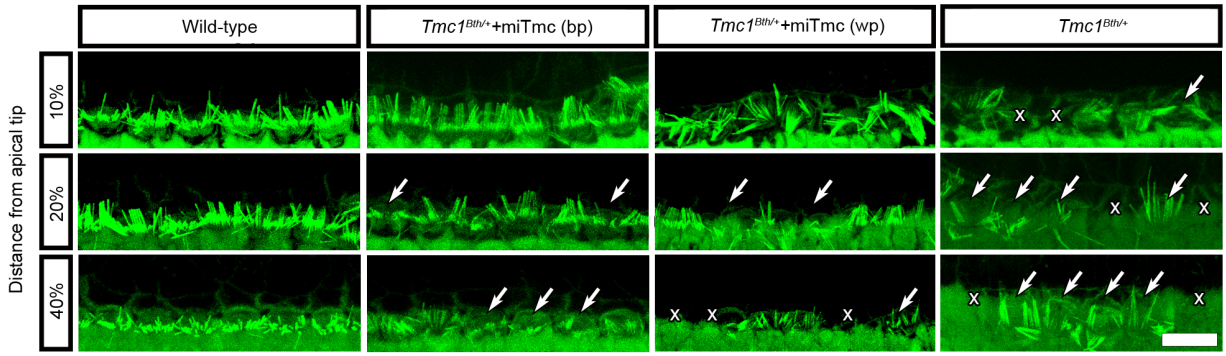

IHC stereocilia bundle morphology in wild-type, *Tmc1*$^{Bth/+}$+miTmc and *Tmc1*$^{Bth/+}$ animals at the indicated percent distance from the apex. Samples are labeled with anti-phalloidin to label F-actin (green). White crosses show absent IHCs, arrows show distorted or splayed stereocilia bundles. Note the number of distorted stereocilia bundles increases in an apex-to-base gradient (20 and 40%). *Tmc1*$^{Bth/+}$+miTmc at 10% shows comparable morphology to wild-type. Scale bar represents 10 μm.

Supplementary Table

Table S1: miRNA designs targeting the mutant *Tmc1* c.1235A allele

miRNA name	Position	Target Site Sequence (sense)	Guide strand (antisense) 21nt (position underlined)
miTmc1K412.5	5	AATGTCCCTCCTGGGGAAGTT	AACTTCCCCAGGAGGGACATT
miTmc1K412.6	6	ATGTCCCTCCTGGGGAAGTTC	GAACTTCCCCAGGAGGGACAT
miTmc1K412.7	7	TGTCCCTCCTGGGGAAGTTCT	AGAACTTCCCCAGGAGGGACA
miTmc1K412.8	8	GTCCCTCCTGGGGAAGTTCTG	CAGAACTTCCCCAGGAGGGAC
miTmc1K412.9	9	TCCCTCCTGGGGAAGTTCTGT	ACAGAACTTCCCCAGGAGGGA
miTmc1K412.10	10	CCCTCCTGGGGAAGTTCTGTC	GACAGAACTTCCCCAGGAGGG
miTmc1K412.11	11	CCTCCTGGGGAAGTTCTGTCC	GGACAGAACTTCCCCAGGAGG
miTmc1K412.12	12	CTCCTGGGGAAGTTCTGTCCC	GGGACAGAACTTCCCCAGGAG
miTmc1K412.13	13	TCCTGGGGAAGTTCTGTCCCA	TGGGACAGAACTTCCCCAGGA
miTmc1K412.14	14	CCTGGGGAAGTTCTGTCCCAC	GTGGGACAGAACTTCCCCAGG
miTmc1K412.15	15	CTGGGGAAGTTCTGTCCCACC	GGTGGGACAGAACTTCCCCAG
miTmc1K412.16	*16	TGGGGAAGTTCTGTCCCACCC	GGGTGGGACAGAACTTCCCCA
miTmc1K412.17	17	GGGGAAGTTCTGTCCCACCCT	AGGGTGGGACAGAACTTCCCC
miTmc1K412.18	18	GGGAAGTTCTGTCCCACCCTG	CAGGGTGGGACAGAACTTCCC
miTmc1K412.19	19	GGAAGTTCTGTCCCACCCTGT	ACAGGGTGGGACAGAACTTCC

Fifteen small interfering RNAs targeting the Beethoven allele of *Tmc1* were designed and embedded in a miRNA expression cassette. These miRNAs were screened *in vitro* in COS-7 cells, assessing suppression of the *Tmc1* c.1235A allele by real-time qPCR of cells co-transfected with a *Tmc1* c.1235A plasmid and miRNA expression cassette plasmids. Asterisks represent siRNA candidates with robust silencing of *Tmc1* c.1235A. miRNAs were designed as described by Boudreau and colleagues [1].

Supplementary References

1. Boudreau, R.L., Spengler, R.M., and Davidson, B.L. (2011). Rational design of therapeutic siRNAs: minimizing off-targeting potential to improve the safety of RNAi therapy for Huntington's disease. Mol Ther 19, 2169-2177.